

## Accepted manuscript

Opalic, S. M., Goodwin, M., Lei, J., Nielsen, H. K., Pardiñas, Á. Á., Hafner, A., Kolhe, M. L. (2020). ANN modelling of CO<sub>2</sub> refrigerant cooling system COP in a smart warehouse. Journal of Cleaner Production, 260, 1-10. <https://doi.org/10.1016/j.jclepro.2020.120887>

Published in: Journal of Cleaner Production

DOI: <https://doi.org/10.1016/j.jclepro.2020.120887>

AURA: <https://hdl.handle.net/11250/3058108>

Copyright: © 2020 Elsevier Ltd.

License: CC BY NC ND

Embargo: Available from 19.03.2022

# ANN modelling of CO<sub>2</sub> refrigerant cooling system COP in a smart warehouse

Sven Myrdahl Opalic<sup>a,b,d,\*</sup>, Morten Goodwin<sup>a,b</sup>, Lei Jiao<sup>a,b</sup>, Henrik Kofoed Nielsen<sup>b</sup>, Ángel Álvarez Pardiñas<sup>c</sup>, Armin Hafner<sup>c</sup> and Mohan Lal Kolhe<sup>b</sup>

<sup>a</sup>Centre for Artificial Intelligence Research, University of Agder, 4879, Grimstad, Norway

<sup>b</sup>Faculty of Engineering and Science, University of Agder, 4879, Grimstad, Norway

<sup>c</sup>Department of Energy and Process Engineering, Norwegian University of Science and Technology, Kolbjorn Hejes vei 1B, 7034, Trondheim, Norway

<sup>d</sup>Login Eiendom AS, Kongens Gata 16, 7011, Trondheim, Norway

## ARTICLE INFO

### Keywords:

Industrial cooling systems  
Carbon dioxide refrigerant  
Artificial neural networks  
Coefficient of performance  
Energy storage  
Smart warehouse

## ABSTRACT

Industrial cooling systems consume large quantities of energy with highly variable power demand. To reduce environmental impact and overall energy consumption, and to stabilize the power requirements, it is recommended to recover surplus heat, store energy, and integrate renewable energy production. To control these operations continuously in a complex energy system, an intelligent energy management system can be employed using operational data and machine learning. In this work, we have developed an artificial neural network based technique for modelling operational CO<sub>2</sub> refrigerant based industrial cooling systems for embedding in an overall energy management system. The operating temperature and pressure measurements, as well as the operating frequency of compressors, are used in developing operational model of the cooling system, which outputs electrical consumption and refrigerant mass flow without the need for additional physical measurements. The presented model is superior to a generalized theoretical model, as it learns from data that includes individual compressor type characteristics. The results show that the presented approach is relatively precise with a Mean Average Percentage Error (MAPE) as low as 5 %, using low resolution and asynchronous data from a case study system. The developed model is also tested in a laboratory setting, where MAPE is shown to be as low as 1.8 %.

## 1. Introduction


The building and construction sector, including energy intensive food distribution warehouses, is responsible for almost 40 % of total emissions related to energy and process (IEA, 2019a). Within the built environment, cooling demand is continually increasing as the weather grows warmer and a larger part of the worlds population and industrial enterprises gain access to air conditioning equipment and cooled building space (IEA, 2019b). The environmental impact of this trend can mainly be alleviated through a two-fold focus on energy efficient operation (Li et al., 2020; Zhu et al., 2019) and use of increasingly viable environmentally friendly refrigerants, such as carbon dioxide (CO<sub>2</sub>), in the Cooling Systems (CS) (Mohammadi and McGowan, 2019; Sarkar et al., 2004; Neksa, 2002; Neksa et al., 1998).

Typically, in warehouses and distribution centers, comprehensive CSs are responsible for a big portion of the building's energy use. CS performance will also be affected by changes in the operational environment, including weather conditions, logistical operations, and workforce behavior (Chua et al., 2010; Sarkar et al., 2004). These effects are enhanced when dealing with environmentally friendly refrigerants, such as CO<sub>2</sub>, that recently have seen an increase in utility due to environmental concerns (Schmidt et al., 2019). A cost efficient way to reduce environmental impact in the existing CSs is through energy efficient operation. This can be achieved in several ways, depending on the existing energy system design,

such as optimized interaction with a Thermal Energy Storage (TES) (Široký et al., 2011), surplus heat recovery (Chua et al., 2010) and optimized time-of-use with simultaneous access to local renewable energy resources (Wu and Wang, 2018; Kow et al., 2018). Implementing an Intelligent Energy Management System (IEMS) allows the building operator to automate the process of continuously choosing actions with the highest cost-reduction or energy-savings potential (T et al., 2018; Venayagamoorthy et al., 2016; Wen et al., 2015; Zhao et al., 2013; Chen et al., 2011). The IEMS takes advantage of the shift from Human-to-Machine to Machine-to-Machine communication, with access to large quantities of data through Internet/Intelligence of Things (IoT) components, and can incorporate the latest developments within Artificial Intelligence (AI) for prediction and control purposes (Hakimi and Hasankhani, 2020; Wu and Wang, 2018; Manic et al., 2016). The IEMS can handle various tasks, such as optimized utilization of energy storage options to reduce overall CS energy consumption (Široký et al., 2011). TES systems can be used to enhance the CS performance by exploiting available heating and cooling capacity for optimum operation of energy storage during high-performance operating conditions. In a CS, the most important energy efficiency measure is the Coefficient of Performance (COP). The COP is a ratio of the useful thermal energy provided compared to the electrical work required. To determine the thermal component of this ratio in direct expansion systems that use the refrigerant for cooling energy distribution, we need an accurate measure of refrigerant flow.

Installing flow measuring equipment in existing CO<sub>2</sub> re-

\*Corresponding author.

 sven.opalic@uia.no (S.M. Opalic)

ORCID(s):

refrigerant, direct expansion CSs is a costly and complicated operation. The complexity and risk increases when the CS operates on multiple temperature levels with separate distribution systems. The most logical option for performance evaluation then becomes a theoretical calculation based on available operational data. In Zou and Xie (2017), a simplified model for COP modelling of a water source heat pump is suggested. Sun et al. (2017) proposes a general simulation model based on graph theory that utilizes accurate mathematical models of individual components, such as the Li (2013) suggested approach to variable speed compressors, to model refrigerant flow. Kim et al. (2018) conducted a case study of variable refrigerant flow simulation, tailored for building energy modelling, where the focus was calibration of a CS model to the U.S. DOE's EnergyPlus software. Zhu et al. (2013) proposes a generic model for variable refrigerant flow in air conditioning systems with multiple evaporators intended for simulation of performance and control analysis. None of the aforementioned studies propose models for multi-stage compression CS. Adaptation and implementation of the proposed methods would also require quite extensive knowledge of refrigeration technology and specific system design. Future IEMS systems might be dependant upon a realistic simulated environment to enable training of sophisticated Reinforcement Learning agents (Schrittwieser et al., 2019; Silver et al., 2018) that can adapt to and learn from operational data. A robust method that allows for cost effective, real-world implementation in complex, industrial scale, CO<sub>2</sub> direct expansion CS is needed. Since industrial scale CSs have to be specifically designed and built for each use case, a general calculation will be quite inaccurate. Intellectual Property (IP) rights tied to the individual components in the CS can also restrict options for full access to precise performance data. Some industrial CS suppliers provide access to web-based software designed for product selection and simple, static performance calculation, but the details necessary to build a more robust theoretical calculation model are not shared. An open, accurate, scalable, and reliable method for theoretical COP calculation is therefore needed.

Within the field of AI, an Artificial Neural Network (ANN) is a particularly powerful tool for hidden function approximation. ANNs trained on limited experimental data were successfully used for COP calculation in Esena et al. (2008). In Opalic et al. (2019) we showed that ANNs trained to model the electrical power utilized by Bitzer, a widely utilized compressor manufacturer, 4CSL12K compressors give highly accurate results, with an MSE of 0.08%, when compared to results attained from Bitzer software.

In this paper, we expand our scope by using ANNs to model all Bitzer compressors in a large and fully operational CO<sub>2</sub>-based CS. To further examine the usefulness and real-world application of this approach, we compare electrical power measurements of a case study CS to the summed calculations of an ensemble of ANNs that each model a compressor type featured in the CS. We also verify our method by comparing our calculations to measurements from a comparable laboratory CS. We train the ANNs using available data

collected from the compressor manufacturer's web-based software. The ANN training algorithm adjusts the weighting of the input parameters, as well as the weighted connections between neurons, to expertly fit the labeled training data. After we define the appropriate input and output parameters, our approach only requires limited knowledge of refrigeration technology and system design to be implemented in an operational setting. In CSs with access to a limited amount of desired performance measures, our approach can be used to supplement and enhance the value of the existing data. In such installations, the overlap between measurements and calculations can also be used to discover inconsistencies between theoretical and actual performance. To the best of our knowledge, our approach to linking theory and practice in multi-stage, CO<sub>2</sub> refrigeration technology using ANNs has not been attempted before. The proposed method is both practically feasible and useful in evaluating the energy performance of CO<sub>2</sub>-based cooling installations. Owners and operators can use our ANN model ensemble approach for quality assurance of CO<sub>2</sub>-based CSs.

We have designed our approach to:

- independently model the parts of the CS that interact with the TES at any given time, such that we can use the efficiency of this isolated part of the CS as input to an algorithm that optimizes the use of the TES;
- have a more accurate performance measure than what is currently available;
- create a data set that enables the development of CS future performance prediction models by applying our method to historical CS data;
- be able to calculate historical values of available excess heat, whereas what is currently known is only the amount of heat that was reclaimed and used;
- investigate to what extent ANNs can model complex scenarios consisting of several cooling compressors in a multi-stage CS – especially including transcritical conditions for CO<sub>2</sub>.

We organize this article in the following manner. Section 2 describes the components of a real-world advanced warehouse and logistical center that includes a case study cooling system, as well as the data collection process for model development. We present our CS model ANN architecture in Section 3. Section 4 is our discussion of results and implementation. Lastly, we present our conclusions and suggest future research efforts in Section 5.

## 2. System structure and configuration

We based our work on information and data collected from a warehouse and food distribution center near Stavanger in Norway, completed in the fall of 2017. The main component of the warehouse energy system is an industrial CO<sub>2</sub> refrigerant CS consisting of three separate cooling plants circulating liquid CO<sub>2</sub> to evaporators in the frozen and chilled

**Table 1**  
Warehouse dimensions and temperatures.

Area	Size	Operating temperature
Dry storage, office space, etc.	19,000 m <sup>2</sup>	18-22°C
Frozen	3,000 m <sup>2</sup>	-20°C
Chilled	3,500 m <sup>2</sup>	0-4 °C
Chilled distribution	3,500 m <sup>2</sup>	0-4 °C

**Table 2**  
Components' specifications.

Component	Capacity	Unit of measurement
PV - photovoltaic power generation	1,000	[kW <sub>p</sub> ]
LBS - lithium-ion battery system	460/200	[kWh/kW]
TES - thermal energy storage	300/300	[m <sup>3</sup> /kW <sub>thermal</sub> ]
CS - cooling system	1,140	[kW <sub>thermal</sub> ]

food storages. The CS also produces chilled water for cooling of the remaining building areas, including food storage, office space, and support areas. The architecture of the case-study cooling plant examined in this study is shown in Fig. 2. An additional back-up and peak-load cooling machine also provides chilled water for ventilation and server cooling. CS surplus heat is recovered and utilized to heat tap water, to keep the ground beneath the frozen storage frost-free and to supply the non-cooled areas of the building with heating energy when needed. If there is insufficient excess heat available, the operating pressure of the CS is increased to satisfy the heating demand, up to a predefined maximum pressure level. Recovered heat can also be stored in a TES for future use, mainly to reduce the need for the electrical boiler at peak heating demand.

The warehouse also exhibits a considerable photovoltaic (PV) power generation plant, a lithium-ion battery system (LBS), and a buried and insulated 300 m<sup>3</sup> firewater tank connected to a heat exchanger that is utilized as a TES. An electrical boiler is employed for back-up and peak demand heating. Table 1 contains a list of the operational temperature range in the various warehouse areas, whereas Fig. 1 and Table 2 visualizes and lists the main components of the warehouse energy system. The PV plant supplies A/C power directly to the main switchboard. If demand is sufficient, all the PV energy is utilized in the building. Otherwise, energy is stored in the LBS, converted to thermal energy and stored in the TES or exported to the main grid. In addition to storing surplus solar energy, the LBS is used for power peak reduction. Thermal energy in the form of chilled or heated water can be stored in the TES, represented by the purple arrow in Fig. 1. The IEMS tasked to control the energy storage systems applies proven machine learning algorithms to predict PV power generation, as well as the future demand for thermal and electrical energy. An optimization algorithm then employs the predictions to calculate the most cost-effective hourly schedule for charging and discharging.

The IEMS controls the TES in two separate seasonal

modes of operation, Heat Energy Storage (HES) and Cold Energy Storage (CES). It employs CES mode from around March to November, and HES for the remainder of the year. Natural reduction of the cooling demand occurs as outside temperature decreases towards the winter season. As a result, surplus heat available for recovery is no longer able to sustain the warehouse's overall demand for heating. However, by storing heating energy reclaimed from the CS in advance, the load on the electric boiler can be severely reduced, which in turn reduces the consumption of energy and the cost of peak power.

In CES mode, the IEMS attempts to balance two main strategies:

1. Storing surplus electricity generated by the PV installation in the CES through energy conversion.
2. Producing and storing chilled water at high COP conditions.

When the IEMS applies strategy number one, the CS converts surplus electricity to chilled water for storage in the CES at a temperature range between 7°C and 15°C. In the evening, when the natural reduction of power output from the PV-plant occurs, the IEMS may choose to discharge the CES and thereby reducing power requirements for the CS. The second strategy involves optimizing the production of cooling energy by decoupling it from the consumption through the CES. The IEMS optimization algorithm accomplishes this through the utilization of cooling demand predictions, weather predictions, and table base COP values.

The IEMS currently uses a simplified approach with a provided table of COP values to evaluate performance at given ambient temperature and operating conditions. Future COP values can then be estimated using weather predictions. The COP table is a rough metric that does not supply the optimization algorithm with quantitative input, such as expected cooling production at the separate CS stages and total available excess heat. Also, the Building Management System (BMS) provides a general CO<sub>2</sub> CS model that calculates all the necessary parameters, but with unsatisfactory accuracy.

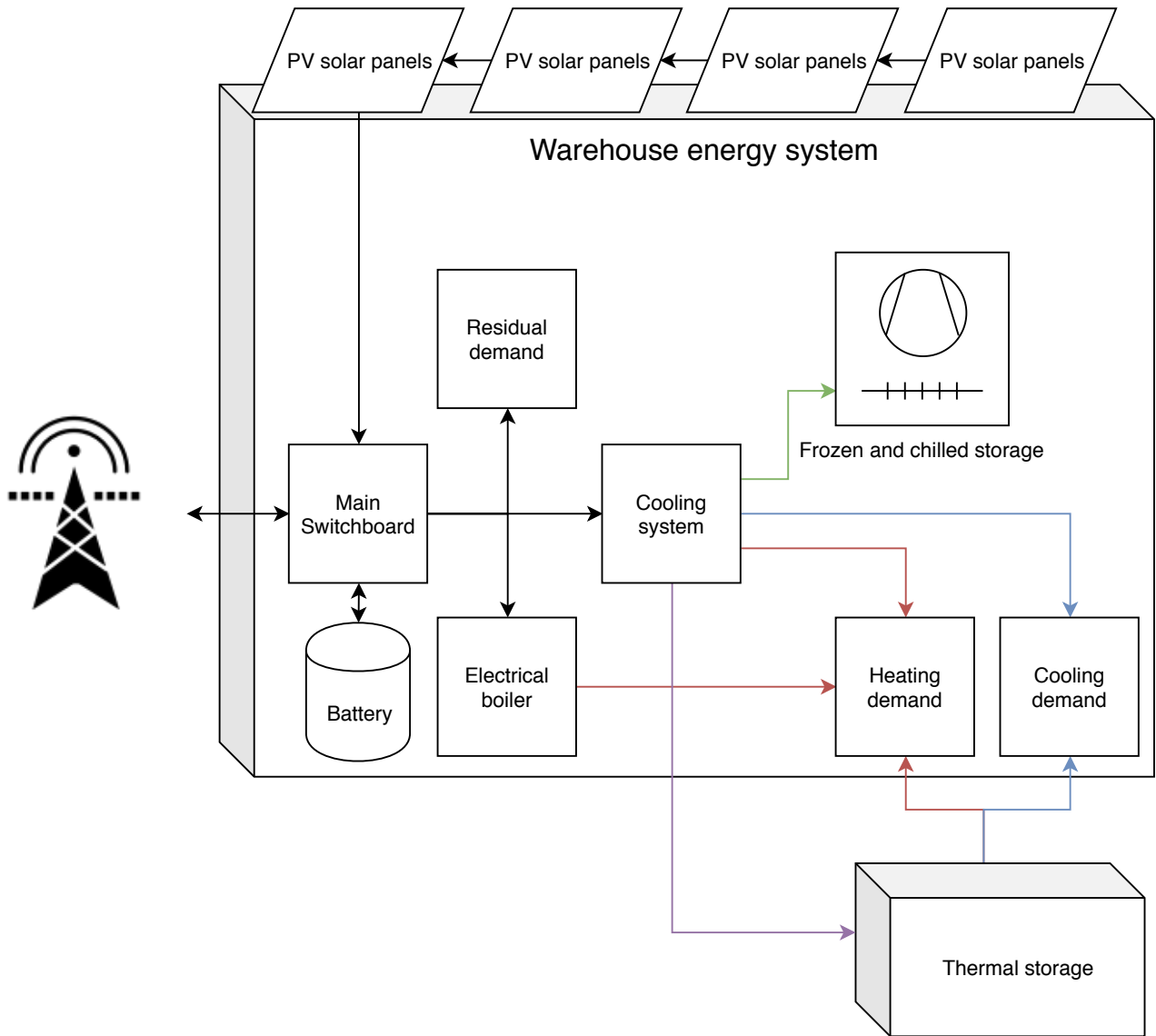


**Figure 1:** The warehouse energy system.

We, therefore, suggest an ANN approach to calculate compressor mass flow and electricity consumption. Calculating cooling capacity instead of mass flow would be preferable. However, due to unavailability of cooling capacity data for all the compressors, we use mass flow as an alternative approach. We have developed models for all the compressors in the cooling system. Two models have been developed for each transcritical compressor so that we use separate models of the same compressor for calculations in the subcritical and transcritical operational modes. The compressors are semi-hermetic reciprocating compressors manufactured by Bitzer GmbH, with one frequency-controlled compressor at each stage. Fig. 2 shows the placement of all the compressors in a simplified cooling system architecture. There are two pressure stages of compression as well as parallel compressors to handle flash gas in the receiver and chilled water production. The compressors for the frozen storage areas are displayed in the bottom left, with the cold storage compressors in the top

left and the parallel compressors in the top right. Fig. 2 also displays mass flow direction and the most crucial CS components. It can be noted that the CO<sub>2</sub> based cooling system is a highly complex part of the energy system in the considered technologically advanced warehouse. Fig. 2 is an element of Fig. 1.

The website of the manufacturer was used to collect data (Bitzer-GmbH, 2019). Theoretical values for cooling capacity ( $Q$ ), electrical power ( $P$ ), electrical current ( $I$ ) or mass flow ( $\dot{m}$ ), which can all be substituted for the parameter  $y$  in Eqs. 1 and 2, can then be separately calculated by using the appropriate constants  $c_i, \forall i \in 1, 2, \dots, 10$  in the following polynomials (according to EN 12900:2013), for subcritical pressure conditions

$$y_{sc} = c_1 + c_2 t_o + c_3 t_c + c_4 t_o^2 + c_5 t_o t_c + c_6 t_c^2 + c_7 t_o^3 + c_8 t_c t_o^2 + c_9 t_o t_c^2 + c_{10} t_c^3,$$

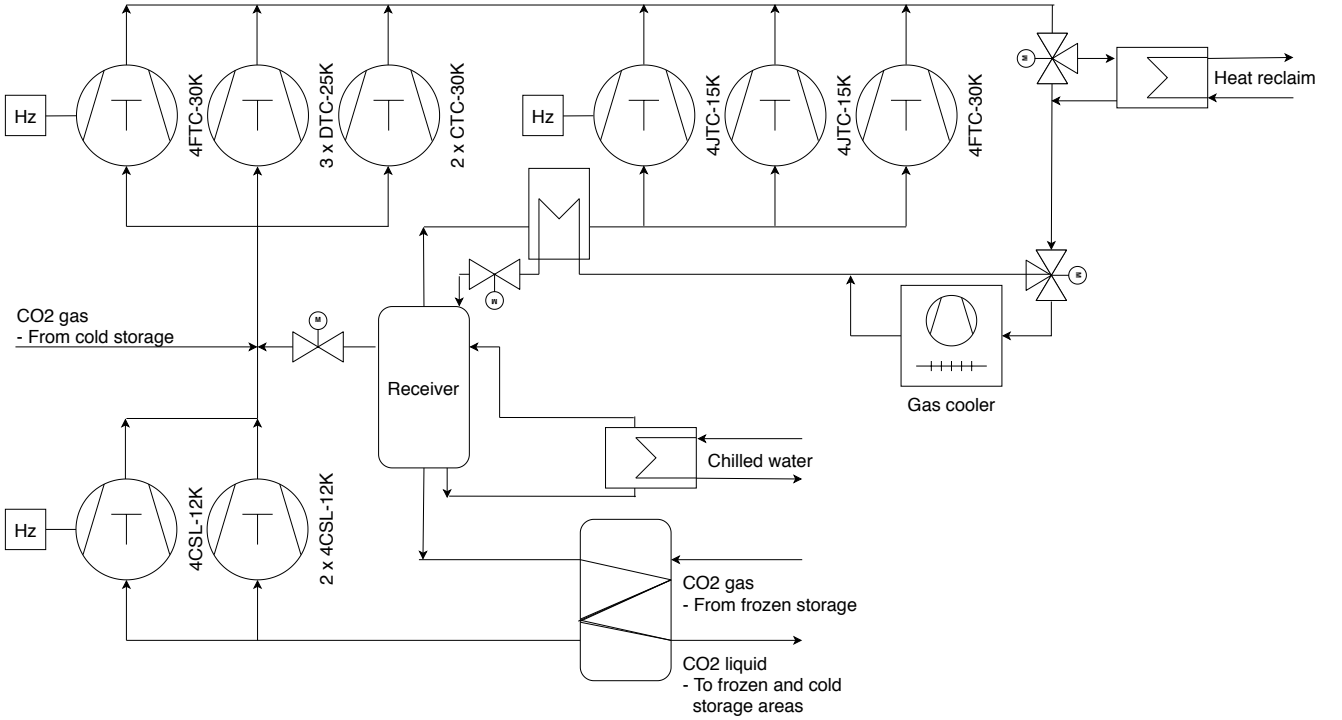


Figure 2: On-site cooling plant architecture.

and, for transcritical pressure

$$y_{tc} = c_1 + c_2 t_o + c_3 p_{HP} + c_4 t_o^2 + c_5 t_o p_{HP} + c_6 p_{HP}^2 + c_7 t_o^3 + c_8 p_{HP} t_o^2 + c_9 t_o p_{HP}^2 + c_{10} p_{HP}^3 \quad (2)$$

In Eqs. (1) and (2),  $t_o$  (°C) is representing temperature of evaporation and  $t_c$  (°C) is the condensation temperature, whereas  $p_{HP}$  [bar] is the discharge pressure of the compressors at transcritical operating conditions where  $p_{HP} > 73.77$  [bar]. The constants  $c_1$  through  $c_{10}$  depend on suction gas temperature (SGT, °C) and compressor operating frequency (CF, Hz) for subcritical operating conditions, while gas cooler outlet temperature (GOT, °C) must also be selected for transcritical operation. Separate and independent sets of constants are used to calculate  $Q$  (kW<sub>thermal</sub>),  $P$  (kW),  $I$  (A) or  $\dot{m}$  (kg/h) when used with Eqs. (1) and (2). Constants for  $P$  and  $\dot{m}$  were collected in 5 degree steps for SGT and GOT within each compressors defined operational range, and 5 Hz steps for CF between 70 and 30 Hz.  $P$  and  $\dot{m}$  example values were then calculated and labelled appropriately using integers for  $t_o$ ,  $t_c$  and  $p_{HP}$ , resulting in data sets ranging from approximately 10 000 to 100 000 training examples for each compressor model.

Finally, we can determine cooling production, available excess heat, and the COP of any part of the system through calculations. For example,  $\dot{m}$  can be used to calculate cooling load with the enthalpy difference equation

$$Q_c = \frac{\dot{m} \Delta h_c}{3600}, \quad (3)$$

where  $\Delta h_c$  (kJ/kg) is the specific enthalpy difference of the refrigerant between the outlet and inlet of a specific evaporation stage. Pressure and temperature of the subcooled liquid refrigerant before the expansion device (evaporator inlet conditions), along with the pressure and temperature of the superheated gas (evaporator outlet conditions), are measured. Specific enthalpy at the inlet and outlet of the evaporation stage is therefore known and can be used to calculate the specific enthalpy difference. We can then calculate the  $COP_c$  of a single, or multiple, compressor(s) using Eq. (4)

$$COP_c = \frac{Q_c}{P}. \quad (4)$$

### 3. ANN approach design and configuration

We chose the appropriate ANN design for compressor modelling by analyzing the Bitzer software and the available data. Clearly, in Eqs. (1) and (2), we can observe the characteristics of a polynomial function. Even though the relationship between the input variables and the constants  $c_i$ ,  $\forall i \in 1, 2, \dots, 10$  are unknown, Eqs. (1) and (2) provide important information which we consider an indication of the hidden function we are attempting to approximate with ANNs.

In the considered ANN approach design and configuration, the patterns are discovered by such a function via training the ANN employing a hyperbolic tangent (tanh) activation function (Opalic et al., 2019; Cybenko, 1989). We, therefore, use the most suited neural network architecture

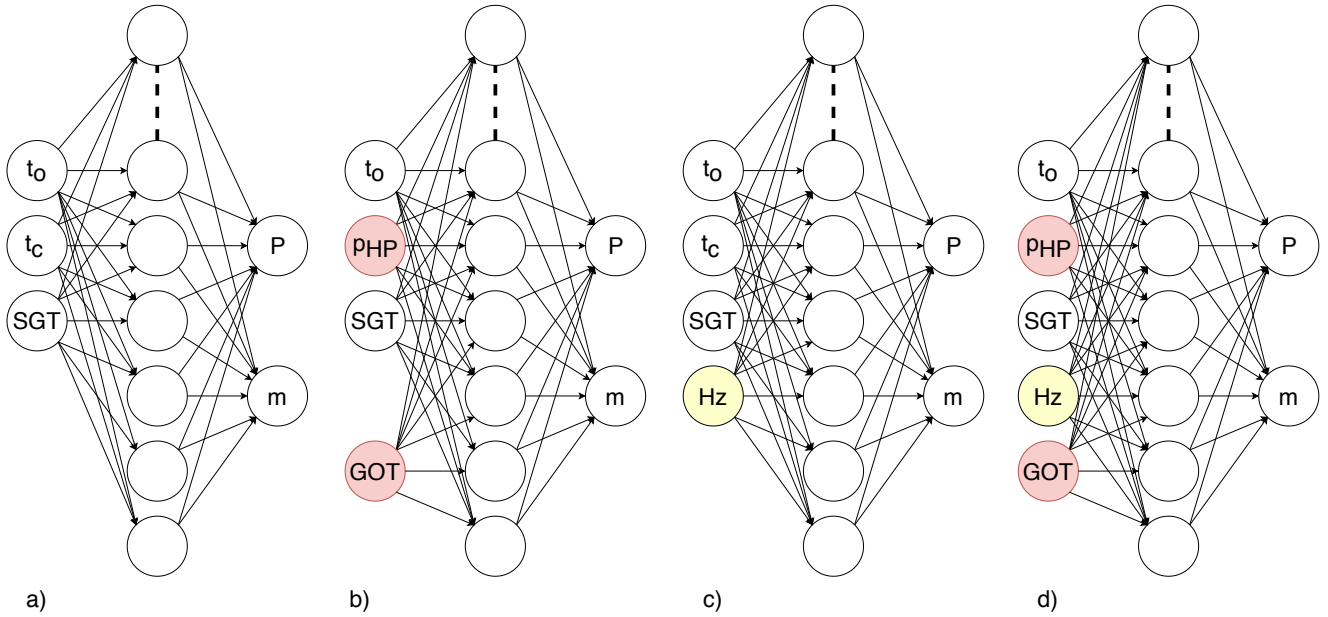


**Figure 3:** ANN model architectures: a) Subcritical operation, b) Transcritical operation, c) Subcritical and frequency controlled, d) Transcritical and frequency controlled.

found in (Opalic et al., 2019), namely using one hidden layer (HL) containing 45 neurons. Fully connected ANNs are configured to calculate  $P$  and  $\dot{m}$  by feed-forwarding input data through the neurons in the HL as shown in Fig. 3. We have trained compressor models for subcritical operating conditions with data sets generated with Eq. (1), while Eq. (2) was utilized to generate the data sets for the transcritical operation model training. The Adam optimizer (Kingma and Ba, 2014) has been applied to update the weights of the neural networks during training. The training continued until model learning converged by using the early-stop method in the Keras (Chollet et al., 2015) programming library, with the "patience" parameter set to 150 epochs.

We set the training optimizer to update the trainable parameters after each training batch, consisting of 100 training examples. We have used Mean Squared Error (MSE) as the loss function while MSE and Mean Average Percentage Error (MAPE) were used as model accuracy metrics.

The models are programmed using Python 3.6 and Keras (Chollet et al., 2015). We divided the data sets into training and validation data through randomization and a factor of 0.9 to 0.1, respectively. We normalized the input values by mean ( $\mu$ ) subtraction and adjusting for variance ( $\sigma^2$ ). The resulting values of  $\mu$  and  $\sigma^2$  calculated on the training data set  $\{X_i\}$  were then employed to also adjust the validation data set.

We finally assembled the individually trained models in accordance with the design of the case-study CS shown in Fig. 2. Operational data from the cooling system was gathered in order to compare the aggregated output of the ANN models for running compressors to the metered power input. In addition to  $t_o$ ,  $t_c$ ,  $P_{HP}$ , SGT, CF and GOT, compressor operating status for each compressor was collected. For every timestep, our algorithm utilizes the operational data to

determine which compressors are operational, the CF of the frequency controlled compressors, and whether the CS pressure level exceeds the transcritical threshold. The data for the active compressors, in the appropriate operational mode, is then selected and sorted into the format shown in Fig. 3, and fed into the input layers of the selected models. The resulting model output is finally summed for each separate stage of compression and compared to the metered power input to the CS.

However, none of the data is temporally synchronized. Accordingly, the raw data had to be processed and aligned in order for comparisons to be made. The data processing introduces an error source that has to be taken into account when observing the results. Also, a third-party BMS, utilizing serial bus communication for data gathering, is responsible for collecting the power measurements and operational data from the cooling system. The BMS only timestamps the data when it is received. There is no timestamp for when the data was requested or when the cooling system controller received the request (the actual time of measurement). This lack of clarity adds another layer of uncertainty to the temporal accuracy and integrity of the raw data. By request, the BMS operator increased the frequency of data collection in June 2019 in order to increase input data quality.

An analysis of the raw data also shows that even when measured power input drops to zero, the BMS will still show active compressors, and accordingly, the models will predict the individual compressor power usage. Therefore, we have removed all data points with a power measurement of zero in the data cleaning process.

An alternative research approach would have been to structure the training data so that a single model could be used to predict the aggregated output. We only briefly consid-

**Table 3**

Training and validation MSE for all models. Separate models for frequency controlled (FC) compressors and transcritical (TC) operation.

Compressor model	Training MSE	Validation MSE
Bitzer 4CSL12K	2,97E-05	2,48E-05
Bitzer 4CSL12K FC	2,37E-05	1,60E-05
Bitzer 4CTC30K	3,90E-05	3,17E-05
Bitzer 4CTC30K TC	7,79E-06	4,57E-06
Bitzer 4DTC25K	1,84E-05	2,01E-05
Bitzer 4DTC25K TC	6,20E-06	2,89E-06
Bitzer 4FTC30K	6,76E-05	6,50E-05
Bitzer 4FTC30K FC	2,68E-05	1,74E-05
Bitzer 4FTC30K FC TC	1,28E-05	7,85E-06
Bitzer 4FTC30K TC	1,54E-05	1,09E-05
Bitzer 4JTC15K	1,87E-05	1,34E-05
Bitzer 4JTC15K FC	2,34E-05	1,82E-05
Bitzer 4JTC15K FC TC	2,19E-05	1,54E-05
Bitzer 4JTC15K TC	7,26E-06	6,91E-06

ered this alternative as such an approach would have included removing known information and system boundaries from the training process only to have the information, hopefully, relearned by the single model. Also, we would have removed the advantage in our chosen approach of being able to model separate stages in the cooling system, while transfer learning by reusing already trained compressor models in other cooling systems would have been more difficult.

There is no flow measuring equipment in the case-study CS that can be used to verify the accuracy of the aggregated model. Therefore, we also tested our method with data from an ongoing experiment at the Norwegian University of Science and Technology (NTNU) laboratory CS. The NTNU CS has a very similar design to the case-study CS, while also measuring the flow of CO<sub>2</sub> through each compressor stage and the individual electrical power input of each compressor. The compressors in the NTNU CS parallel stage, consisting of a Bitzer 2KTE-7K-40S (Inverter driven), Bitzer 2KTE-7K-40S (set to fixed speed) and Bitzer 4JTC-15K-40S (fixed speed), were modeled using our previously described ANN configuration approach. Part of the pressure and temperature sensors in the NTNU CS are connected to Danfoss controllers which sample and log the data in 5-second intervals. Mass flow meters, temperature sensors, and active power consumption meters for the compressors are connected to National Instruments Hardware, and the data is logged by LabVIEW software with a sampling time of 1 second. LabVIEW software also handles information coming from the inverters (frequency, power, etc.), connected by Modbus, with a 5 second sampling time. NTNU researchers finally synchronize all the data in MATLAB with in-house software.

## 4. Results and implementation plan

### 4.1. Results analysis

In this paper, we attempt to model the compressors in an operational, industrial CS using ANNs. We trained the ANNs with data generated by calculating power input and mass flow

of Bitzer CO<sub>2</sub> CS compressors using polynomials, subject to openly available constants, for subcritical and transcritical conditions. The difference between training and validation error, as shown in Table 3, is minimal in all cases. Therefore, we could likely have used a more significant part of the data sets for training without risk of overfitting. Table 3 lists the training and validation MSE results for each compressor model. Table 3 shows that the models are highly accurate when compared to training and validation data sets generated with Eq. (1) and (2) and can therefore be expected to give very similar results to the hidden ground-truth theoretical models.

Table 4 shows results for aggregated model output compared to metered power input to the case study CS every month from January 2019 to July 2019. We observe an increase in aggregated model predictive accuracy compared to power measurements in June and July, which is likely due to the increased data collection frequency implemented in the BMS. Fig. 4 and 5 show monthly plots for the worst (April) and best (July) months. Making any visual distinction between these months is difficult, but an apparent trend in both months is that the largest discrepancies between predicted and actual power input exists in the lower spectrum of power usage. Sudden drops in measured power input, not reflected in the CS BMS data, is a probable cause of this trend. It is therefore likely that there is an error in the raw CS data connected to sudden drops in power input, perhaps due to sudden switches between compressors or a rapid decrease in cooling demand when local evaporator set-point temperature conditions are met. We find further evidence of this when examining the differences between MSE and MAPE in TC or SC operation during warmer or colder months. Table 4 shows that the MSE and MAPE in transcritical operating conditions are higher than in subcritical operation for January through May, while the opposite is true in June and July. Since heat is reclaimed from the CS and used for heating purposes, pressure is increased in the winter months when



**Table 4**

Monthly MSE and MAPE comparison from January 2019 to July 2019. Separate columns for subcritical (SC) and transcritical (TC) operating conditions.

Month	MSE	MSE TC	MSE SC	MAPE	MAPE TC	MAPE SC
January	112.3	120.7	104.1	15.8 %	14.9 %	16.7 %
February	102.8	106.9	101.7	15.4 %	12.4 %	16.2 %
March	90.7	112.0	85.4	14.7 %	13.8 %	14.9 %
April	145.7	187.9	136.3	18.3 %	18.7 %	18.2%
May	88.0	130.9	79.7	16.3 %	18.3 %	15.9 %
June	44.2	34.6	45.5	12.0 %	6.1 %	12.8 %
July	38.8	31.1	42.6	10.1 %	5.8 %	12.3 %

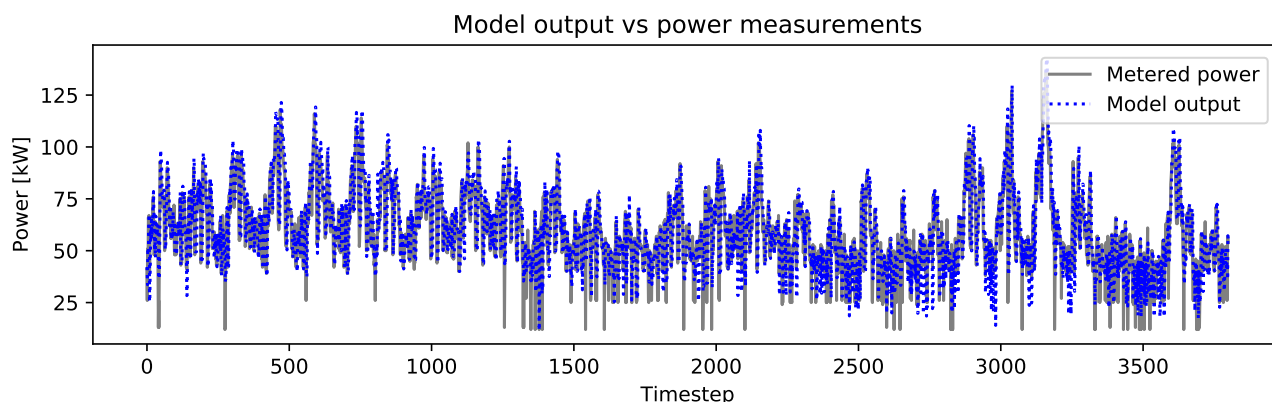


**Figure 4:** April 2019 - Aggregated model output compared with metered power input to CS.

the heating distribution system requests more energy concurrently with or caused by drops in cooling demand. Inversely, during the summer months, pressure increases are usually caused by an increase in ambient temperature and cooling demand. Therefore, the conditions likely to cause the most significant discrepancies occur most often in TC operation in the colder parts of the year and SC operation during the summer, possibly leading to the observable differences in TC and SC MSE and MAPE in Table 4.

Since the monthly plots are quite hard to read due to a large number of data points, we include plots of a single random day in April and July in Fig. 6 and 7. These plots show the importance of the increased quality of the aggregated model input data. Fig.6 indicates a temporal displacement between the aggregated model output and the power measurements when compared to Fig. 7.

Due to the jitters in time for the input data, the model output and the power measurements are not precisely temporally

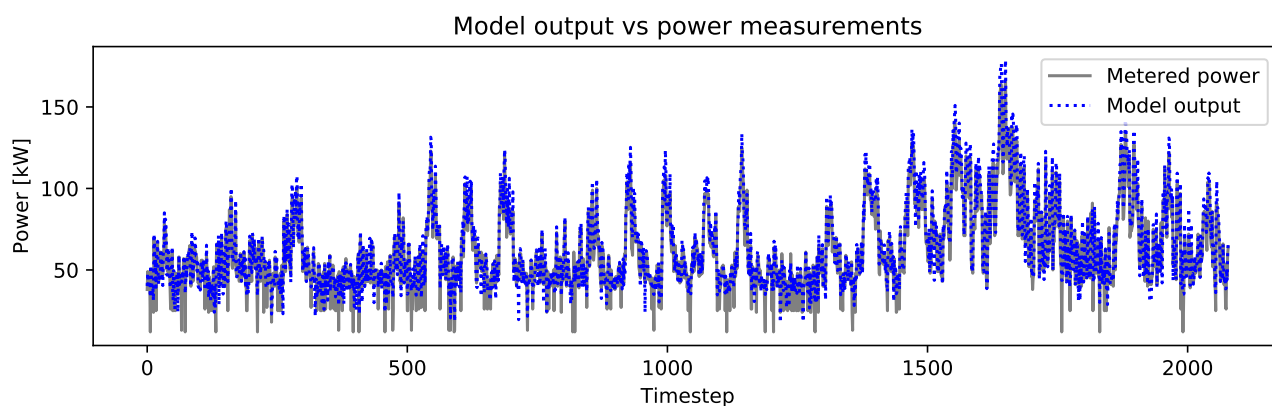


**Figure 5:** July 2019 - Aggregated model output compared with metered power input to CS.

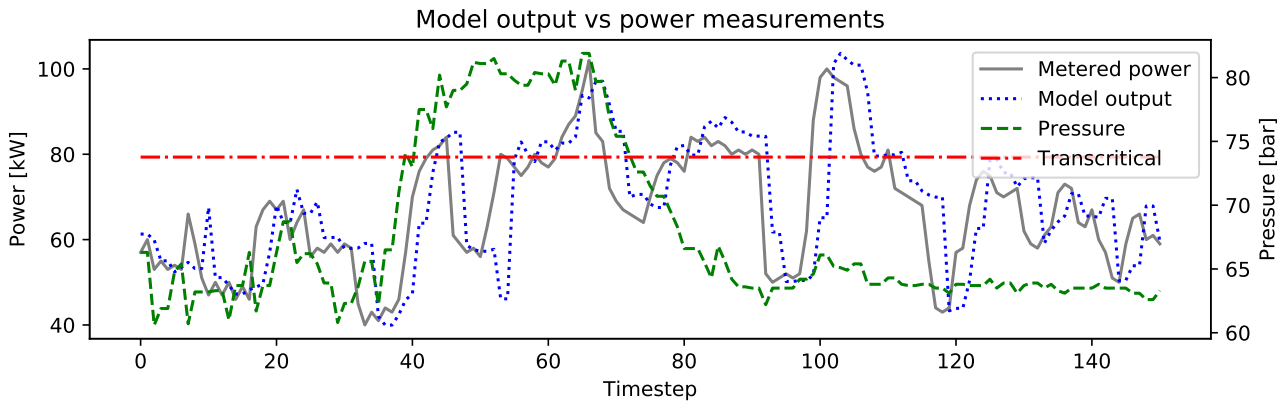


**Figure 6:** 2019-04-10, 24 hours - Aggregated model output compared with metered power input to CS.

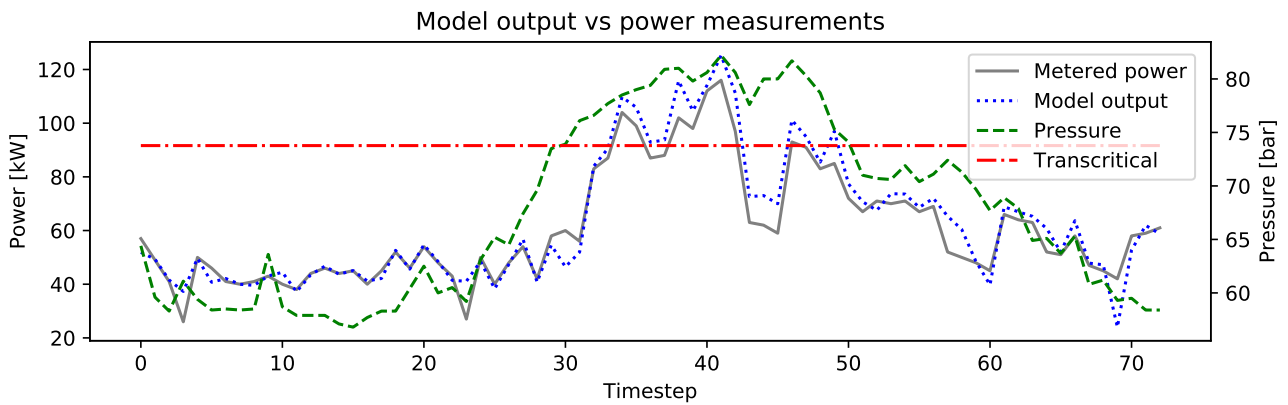


**Figure 7:** 2019-07-16, 24 hours - Aggregated model output compared with metered power input to CS.

aligned. To illustrate and compare the results accordingly, we introduced an offset  $\tau$  in the time domain to align the two data series. In more detail, we shift  $P(t)$  by  $\tau \in [-10, 10]$  to find the maximum output of  $\max_{\tau} \sum_t M(t)P(t + \tau)$ . In this way, we can probably achieve a more appropriate time

alignment.

The maximum was found at  $\tau = -2$ . Adjusting accordingly reduces the MSE in April from 145.7 to 50.5 and the MAPE from 18.3 % to 10.1 %. For 2019-04-10 in Fig. 6 the MSE was reduced from 133.3 to 29.4 and MAPE from 12.8

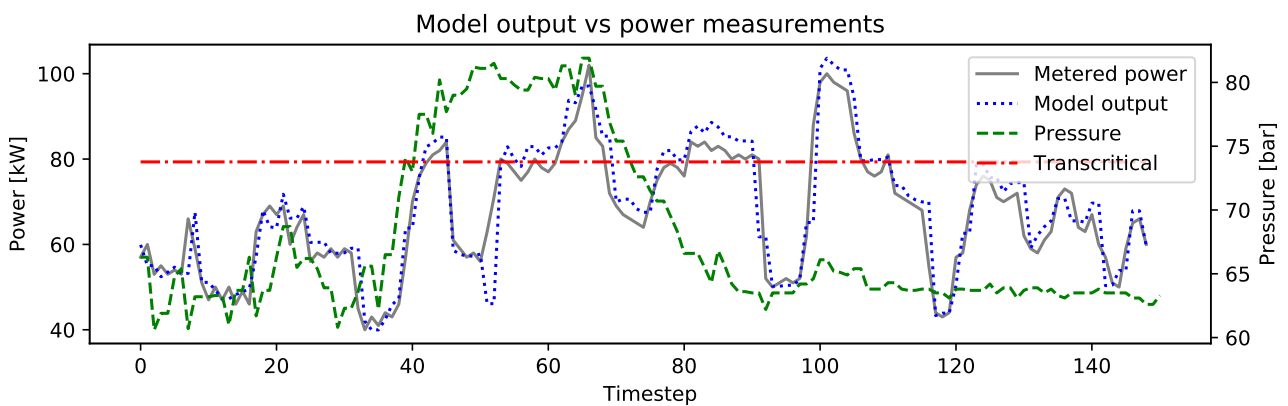


**Figure 8:** 2019-04-10, 24 hours - Aggregated model output compared with metered power input to CS, adjusted for  $\tau = -2$ .

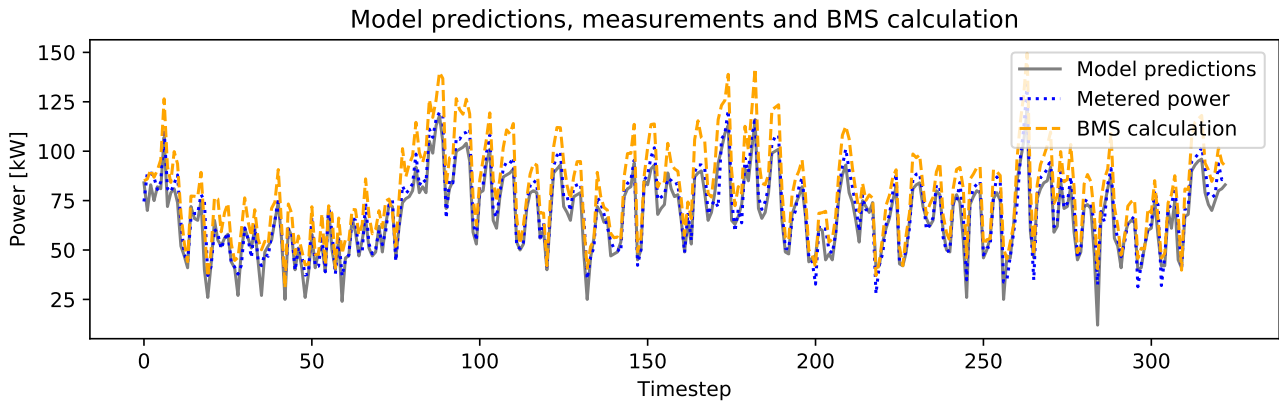


**Figure 9:** 2019-08-22 to 2019-08-26 - Aggregated model output compared with metered power input to CS and BMS calculated values.

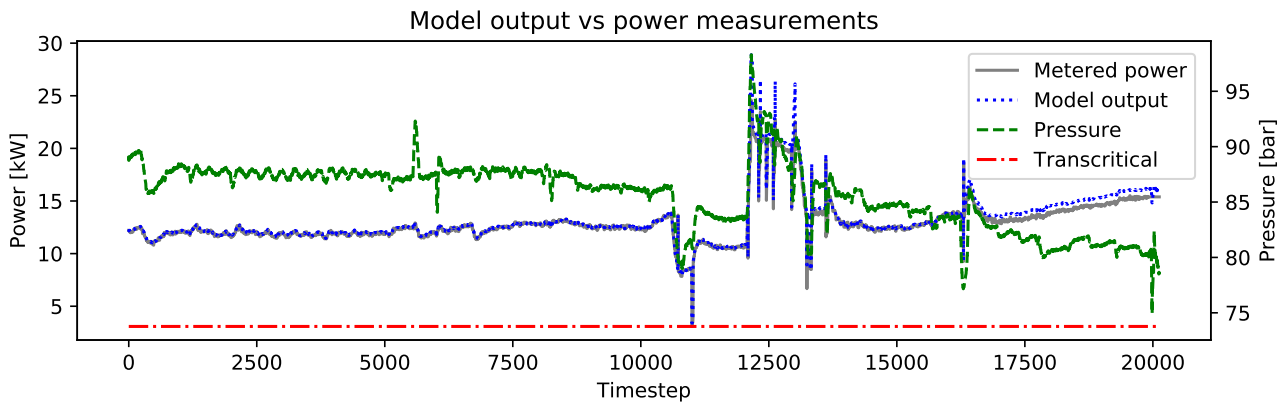


**Figure 10:** 2019-08-25 - Aggregated model power calculation compared with metered power input (inverter) at the NTNU laboratory CS.

% to 5.5 %, results shown in Fig. 8.

We also compare our aggregated model to BMS calculations. BMS calculation parameters were first adjusted to maximize accuracy on 2019-08-22. Results for 2019-08-22

to 2019-08-26 are plotted in Fig. 9. Aggregated model calculation MSE on this sample is 41.7, while the MSE for the BMS calculation is 206.2. Similarly, our model calculation MAPE is 8.5 % compared to 20.1 % for the BMS calculation.

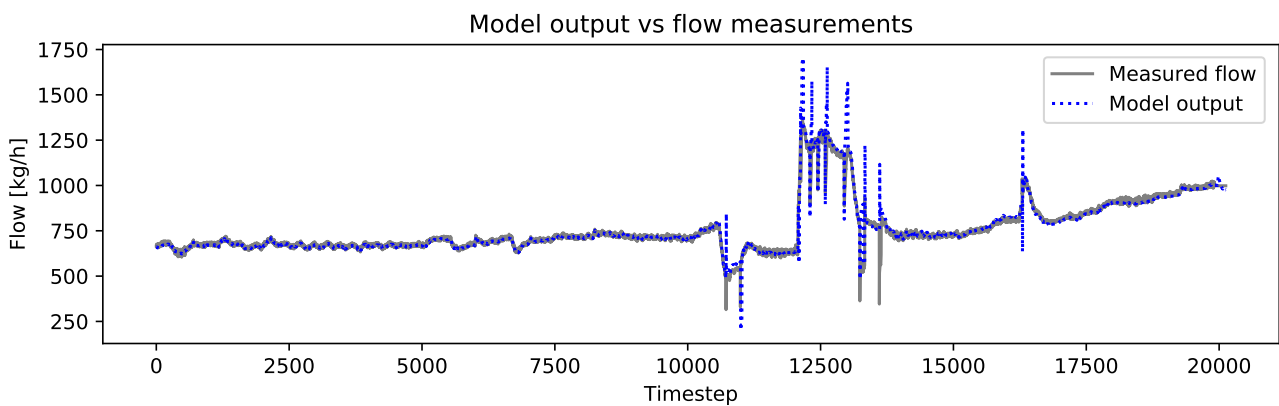


**Figure 11:** 2019-08-25 - Aggregated model flow output compared with measured flow at the NTNU laboratory CS.

Finally, we use data, collected through sensor networks, from an ongoing NTNU CS experiment to validate our approach in a laboratory setting. Measurements of power and flow in the ongoing experiment are compared to the outputs of our aggregated ANN model. The NTNU experiment was conducted in transcritical operating conditions, with pressure ranging from 74.9 bar to 98.3 bar. Results are plotted in Fig. 10 and 11. We obtain a MAPE of 3.13 % when comparing the output from the ANNs with measurements from the power meters, whereas using measurements from the inverter for the frequency controlled compressor reduces MAPE to 1.87 %. Measurements from the power meters includes the power consumption of the inverter as well as power conversion losses. The increased accuracy, when using measurements in the inverter, suggests that the aforementioned losses are not included in the Bitzer software (Bitzer-GmbH, 2019) calculations. The result for the ANN flow output compared to NTNU CS measurements is 1.76 % MAPE. These results show that the presented method is accurate, when given synchronized data with a low sampling time period. Our results also suggest that the underlying ground truth mathematical function for each compressor type could possibly be unknown to the compressor manufacturer. The form that the available data is given in, combined our highly accurate results in a laboratory setting, suggest that the values for the constants could be based on empirical testing of each compressor. If this is the case, our approach could also be a useful way for the compressor manufacturer to easily encode all their laboratory data in neural networks that can be employed in their own calculation software.

#### 4.2. Implementation in the operational setting

Industrial CSs are very power intensive and produce large amounts of surplus heat that is often discarded. In the case study warehouse, excess heat from the CS can be effectively used or stored in the TES to reduce the need for additional heating supplied by the electrical boiler, as described in Fig. 1. Chilled water can be produced and stored in the TES during periods of favorable CS operating conditions and low energy prices, or access to surplus solar energy that would otherwise be exported to the main grid at a severely reduced energy price. The IEMS can facilitate energy management and reduction of the operational demands in an intelligent way to reduce energy cost and environmental impact. To optimize CS and TES interaction, the time-varying performance of the CS is required. The presented ANN model is currently being implemented and configured to supply the IEMS with compressor power consumption and refrigerant mass flow. Our software has been installed at a dedicated local server and communicates directly with the BMS through an Application Programming Interface (API) developed by the BMS provider, utilizing the JSON-RPC 2.0 protocol. The IEMS then collects live data as needed from the BMS through a local gateway setup.

Historical data generated with our ANN ensemble has also been supplied to the IEMS provider to allow development of predictive models of CS performance. The perfor-

mance prediction model is developed with machine learning tools and will be utilized as input to the IEMS optimization algorithm. The output of the presented aggregated ANN model will improve the performance of the smart warehouse IEMS by increasing the quality of its necessary input data. The energy management system operator will also use these measures for quality assurance and performance evaluation through visualization in the Building Energy Management System.

## 5. Conclusions

Industrial cooling systems are responsible for a considerable amount of the buildings total energy use and environmental impact. To reduce energy consumption and conserve the environment, it is recommended to recover and store surplus heat, and optimize system operation for utilizing it in coordination with intermittent renewable energy production. These tasks have to be managed intelligently in a complex energy system with dynamic operation of various sub-systems / components. In this work, we have presented ANN model of an operational CO<sub>2</sub>-based industrial cooling sub-system of a complex warehouse energy system. The operating temperature and pressure measurements, as well as the operating frequency of frequency-controlled compressors, are used in developing the operational model. The output of the model is electrical consumption and refrigerant mass flow for the compression process. The presented technique is relatively superior to a general theoretical model, both in terms of accuracy, flexibility, cost effectiveness, and implementability in the real-world application.

The developed model has MAPE in the range of 5 % to 12 % in the operational case-study cooling system. The presented results also indicate that the accuracy can be drastically improved with increased quality of data collection frequency in the operational measurement, supported by a MAPE of 1.87 % and 1.76 % in a comparable laboratory CS, for power and flow respectively. The accuracy of the presented ANN flow calculations is promising from a practical standpoint, and can be implemented through Machine-to-Machine communication using IoT related devices.

The developed modelling of the cooling system is currently being implemented in the case study energy system (Fig. 1). The energy system operator has already noticed improvement in the performance calculation accuracy. The energy system operator will also use these embedded measures for quality assurance and performance evaluation of the building energy management system. Implementation of our approach in current, and future RL, IEMS solutions should be explored. Additional training of the developed models, based on increasing amounts of operational data, could also be further examined.

## References

- Bitzer-GmbH, 2019. Bitzer software v6.10.2 rev2250. <https://www.bitzer.de/websoftware/Calculate.aspx?cid=1568633079921&mod=HHK>.
- Chen, C., Duan, S., Cai, T., Liu, B., Hu, G., 2011. Smart energy management

- system for optimal microgrid economic operation. *IET Renewable Power Generation* 5, 258–267.
- Chollet, F., et al., 2015. Keras. <https://keras.io>.
- Chua, K., Chou, S., Yang, W., 2010. Advances in heat pump systems: A review. *Applied Energy* 87, 3611–3624.
- Cybenko, G., 1989. Approximation by superpositions of a sigmoidal function. *Mathematics of control, signals and systems* 2, 303–314.
- EN 12900:2013, 2013. Refrigerant compressors - Rating conditions, tolerances and presentation of manufacturer's performance data. Standard. European Committee for Standardization. Brussels, Belgium.
- Esen, H., Inallib, M., Sengur, A., Esena, M., 2008. Performance prediction of a ground-coupled heat pump system using artificial neural networks. *Expert Systems with Applications* 35, 1940–1948.
- Hakimi, S.M., Hasankhani, A., 2020. Intelligent energy management in off-grid smart buildings with energy interaction. *Journal of Cleaner Production* 244, 118906. URL: <http://www.sciencedirect.com/science/article/pii/S095965261933776X>, doi:<https://doi.org/10.1016/j.jclepro.2019.118906>.
- IEA, 2019a. Energy efficiency 2019. <https://www.iea.org/reports/energy-efficiency-2019>.
- IEA, 2019b. Global status report for buildings and construction 2019. <https://www.iea.org/reports/global-status-report-for-buildings-and-construction-2019>.
- Kim, D., Cox, S.J., Cho, H., Im, P., 2018. Model calibration of a variable refrigerant flow system with a dedicated outdoor air system: A case study. *Energy and Buildings* 158, 884–896. URL: <http://www.sciencedirect.com/science/article/pii/S0378778817326385>, doi:<https://doi.org/10.1016/j.enbuild.2017.10.049>.
- Kingma, D.P., Ba, J., 2014. Adam: A method for stochastic optimization. *CoRR abs/1412.6980*. arXiv:1412.6980.
- Kow, K.W., Wong, Y.W., Rajkumar, R., Isa, D., 2018. An intelligent real-time power management system with active learning prediction engine for pv grid-tied systems. *Journal of Cleaner Production* 205, 252–265. URL: <http://www.sciencedirect.com/science/article/pii/S0959652618327884>, doi:<https://doi.org/10.1016/j.jclepro.2018.09.084>.
- Li, L.L., Liu, Y.W., Tseng, M.L., Lin, G.Q., Ali, M.H., 2020. Reducing environmental pollution and fuel consumption using optimization algorithm to develop combined cooling heating and power system operation strategies. *Journal of Cleaner Production* 247, 119082. URL: <http://www.sciencedirect.com/science/article/pii/S0959652619339526>, doi:<https://doi.org/10.1016/j.jclepro.2019.119082>.
- Li, W., 2013. Simplified steady-state modeling for variable speed compressor. *Applied Thermal Engineering* 50, 318–326. URL: <http://www.sciencedirect.com/science/article/pii/S1359431112005649>, doi:<https://doi.org/10.1016/j.applthermaleng.2012.08.041>.
- Manic, M., Amarasinghe, K., Rodriguez-Andina, J.J., Rieger, C., 2016. Intelligent buildings of the future: Cyberaware, deep learning powered, and human interacting. *IEEE Industrial Electronics Magazine* 10, 32–49.
- Mohammadi, K., McGowan, J.G., 2019. A thermo-economic analysis of a combined cooling system for air conditioning and low to medium temperature refrigeration. *Journal of Cleaner Production* 206, 580–597. URL: <http://www.sciencedirect.com/science/article/pii/S0959652618328270>, doi:<https://doi.org/10.1016/j.jclepro.2018.09.107>.
- Neksa, P., 2002. Co<sub>2</sub> heat pump systems. *International Journal of Refrigeration* 25, 421–427.
- Neksa, P., Rekdal, H., Zakeri, G., Schiefloe, P.A., 1998. Co<sub>2</sub>-heat pump water heater: characteristics, system design and experimental results. *International Journal of Refrigeration* 21, 172–179.
- Opalic, S.M., Goodwin, M., Jiao, L., Nielsen, H.K., Kolhe, M.L., 2019. Modelling of compressors in an industrial co<sub>2</sub>-based operational cooling system using ann for energy management purposes, in: Macintyre, J., Iliadis, L., Maglogiannis, I., Jayne, C. (Eds.), *Engineering Applications of Neural Networks*, Springer International Publishing, Cham. pp. 43–54.
- Sarkar, J., Bhattacharyya, S., Gopal, M., 2004. Optimization of a transcritical co<sub>2</sub> heat pump cycle for simultaneous cooling and heating applications. *International Journal of Refrigeration* 27, 830–838.
- Schmidt, D., Singleton, J., Bradshaw, C.R., 2019. Development of a light-commercial compressor load stand to measure compressor performance using low-gwp refrigerants. *International Journal of Refrigeration* 100, 443–453. URL: <http://www.sciencedirect.com/science/article/pii/S0140700719300593>, doi:<https://doi.org/10.1016/j.ijrefrig.2019.02.009>.
- Schrittwieser, J., Antonoglou, I., Hubert, T., Simonyan, K., Sifre, L., Schmitt, S., Guez, A., Lockhart, E., Hassabis, D., Graepel, T., Lillicrap, T., Silver, D., 2019. Mastering atari, go, chess and shogi by planning with a learned model. arXiv:1911.08265.
- Silver, D., Hubert, T., Schrittwieser, J., Antonoglou, I., Lai, M., Guez, A., Lanctot, M., Sifre, L., Kumaran, D., Graepel, T., Lillicrap, T., Simonyan, K., Hassabis, D., 2018. A general reinforcement learning algorithm that masters chess, shogi, and go through self-play. *Science* 362, 1140–1144. URL: <https://science.sciencemag.org/content/362/6419/1140>, doi:10.1126/science.aar6404, arXiv:<https://science.sciencemag.org/content/362/6419/1140.full.pdf>.
- Široký, J., Oldewurtel, F., Cigler, J., Prívar, S., 2011. Experimental analysis of model predictive control for an energy efficient building heating system. *Applied Energy* 88, 3079–3087. URL: <http://www.sciencedirect.com/science/article/pii/S0306261911001668>, doi:<https://doi.org/10.1016/j.apenergy.2011.03.009>.
- Sun, H., Ding, G., Hu, H., Ren, T., Xia, G., Wu, G., 2017. A general simulation model for variable refrigerant flow multi-split air conditioning system based on graph theory. *International Journal of Refrigeration* 82, 22–35. URL: <http://www.sciencedirect.com/science/article/pii/S0140700717302839>, doi:<https://doi.org/10.1016/j.ijrefrig.2017.07.003>.
- T, R., Jasmin, E.A., Ahamed, T.P.I., 2018. Residential load scheduling with renewable generation in the smart grid: A reinforcement learning approach. *IEEE Systems Journal*, 1–12.
- Venayagamoorthy, G.K., Sharma, R.K., Gautam, P.K., Ahmadi, A., 2016. Dynamic energy management system for a smart microgrid. *IEEE Transactions on Neural Networks and Learning Systems* 27, 1643–1656.
- Wen, Z., O'Neill, D., Maei, H., 2015. Optimal demand response using device-based reinforcement learning. *IEEE Transactions on Smart Grid* 6, 2312–2324.
- Wu, N., Wang, H., 2018. Deep learning adaptive dynamic programming for real time energy management and control strategy of micro-grid. *Journal of Cleaner Production* 204, 1169–1177. URL: <http://www.sciencedirect.com/science/article/pii/S0959652618327665>, doi:<https://doi.org/10.1016/j.jclepro.2018.09.052>.
- Zhao, Z., Lee, W.C., Shin, Y., Song, K.B., 2013. An optimal power scheduling method for demand response in home energy management system. *IEEE Transactions on Smart Grid* 4, 1391–1400.
- Zhu, X., Wang, F., Niu, D., Guo, Y., Jia, M., 2019. An energy-saving bottleneck diagnosis method for industrial system applied to circulating cooling water system. *Journal of Cleaner Production* 232, 224–234. URL: <http://www.sciencedirect.com/science/article/pii/S095965261931858X>, doi:<https://doi.org/10.1016/j.jclepro.2019.05.322>.
- Zhu, Y., Jin, X., Du, Z., Fan, B., Fu, S., 2013. Generic simulation model of multi-evaporator variable refrigerant flow air conditioning system for control analysis. *International Journal of Refrigeration* 36, 1602–1615. URL: <http://www.sciencedirect.com/science/article/pii/S0140700713001084>, doi:<https://doi.org/10.1016/j.ijrefrig.2013.04.019>.
- Zou, S., Xie, X., 2017. Simplified model for coefficient of performance calculation of surface water source heat pump. *Applied Thermal Engineering* 112, 201–207. URL: <http://www.sciencedirect.com/science/article/pii/S135943111632378X>, doi:<https://doi.org/10.1016/j.applthermaleng.2016.10.081>.